Blue luminescence in porous anodic alumina films

2007 J. Phys.: Condens. Matter 19 216203

(http://iopscience.iop.org/0953-8984/19/21/216203)

IOP PUBLISHING JOURNAL OF PHYSICS: CONDENSED MATTER

J. Phys.: Condens. Matter **19** (2007) 216203 (7pp) doi:10.1088/0953-8984/19/21/216203

Blue luminescence in porous anodic alumina films

Zhaojian Li and Kelong Huang[1]

College of Chemistry and Chemical Engineering, Central South University, Changsha 410083, People's Republic of China

E-mail: lizhaojian_lzj@hotmail.com and klhuang@mail.csu.edu.cn

Received 5 January 2007, in final form 3 April 2007
Published 27 April 2007
Online at stacks.iop.org/JPhysCM/19/216203

Abstract

We have investigated the luminescence property of anodic alumina membranes (AAM) with ordered nanopore arrays prepared by electrochemically anodizing aluminium in oxalic acid, sulfuric acid and phosphoric acid solutions. The photoluminescence (PL) intensity of AAM prepared in $C_2H_2O_4$ is much higher than that of AAMs prepared in H_2SO_4 and H_3PO_4. The PL spectra obtained show that there are two optical centres for the AAMs prepared in H_2SO_4 and H_3PO_4, of which the first originates from the F^+ centres, and the second is associated with the F centres. It is found that the oxalic impurities incorporated in the AAMs should have important influences on the optical properties of AAM prepared in $C_2H_2O_4$. The blue emission band in the AAM prepared in $C_2H_2O_4$ originates from the coactions of the F^+ centres, the F centre and the luminescent centres transformed from oxalic impurities.

1. Introduction

The structure of AAM has been studied for more than 50 years [1]. Under appropriate anodic oxidation conditions, very regular self-ordered, honeycomb-like hexagonal arrays with a circular pore at the centre of each hexagon can be obtained [2]. It has attracted increasing interest because of its favourable applications as a template in fabricating nanostructures and nanomaterials [2–6]. To study the photoluminescence properties of the AAM itself for practical applications is important, because the properties of the AAM certainly affect the properties of materials based on AAM. However, the physical properties of the porous alumina itself have not been investigated intensively [7]. In recent years, most investigators have focused their attention on the light-emitting properties of the AAM formed in oxalic acid and have revealed the origin of a blue emission [8–13]. Little has been done on the PL properties of AAMs formed in phosphoric acid and sulfuric acid [7, 12, 14]. Therefore, a study of the influence of electrolytes on the optical properties of the prepared AAM film is an essential point for various applications. In this article, we carefully examine the PL properties of the alumina

[1] Author to whom any correspondence should be addressed.

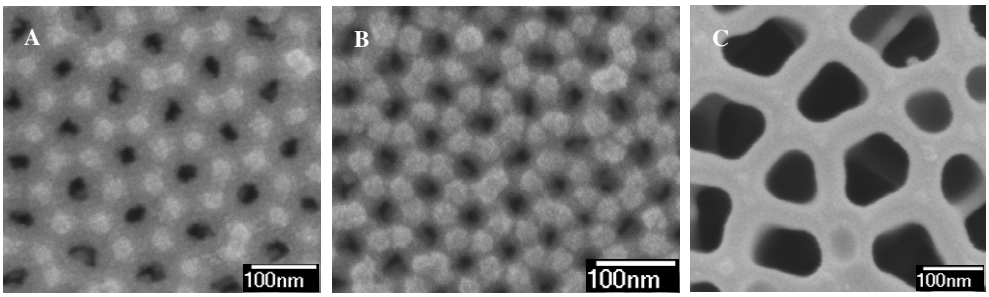

Figure 1. SEM micrograph of surfaces of the AAMs: (A) the AAM_C; (B) the AAM_S; (C) the AAM_P.

membranes formed in oxalic acid, sulfuric acid and phosphoric acid solutions. Mechanisms of the photoluminescence and characterization behaviours of the PL were discussed. This work improves the understanding of the light-emitting mechanism in the alumina membranes.

2. Samples and experiments

The AAMs were fabricated through a typical two-step anodizing electrochemical procedure [2] with high-purity (99.99%) aluminium foil as the anode. After annealing at 500 °C for 23 h, an aluminium foil was degreased in acetone and electro-polished in a mixture of EtOH (80 vol%) and $HClO_4$ (20 vol%). The aluminium foil was anodized in 0.3 M oxalic acid (denoted as AAM_C), 10% (v/v) phosphoric acid (denoted as AAM_P) and 0.3 M sulfuric acid (denoted as AAM_S) electrolyte, respectively. The anodizing voltage was 40 V for $C_2H_2O_4$, 25 V for H_2SO_4 and 60 V for H_3PO_4, respectively. The temperature of the electrolyte was kept constant at 11 °C for $C_2H_2O_4$ and 6 °C for H_3PO_4 and H_2SO_4, respectively. The specimens were then immersed in a mixture of 6.0 wt% H_3PO_4 and 1.8 wt% H_2CrO_4 at 60 °C for 1 h to remove the alumina layers. Then, the aluminium foil was anodized again for 3 h under the same conditions as the first step. The remaining aluminium of the porous alumina was removed in a $CuCl_2$-based solution (100 ml of HCl (38%) + 100 ml H_2O + 3.4 g of $CuCl_2{\cdot}2H_2O$). The morphologies of the samples were investigated using a JEOL JSM-6360LV scanning electron microscope (SEM). The PL spectral measurements were carried out on a Hitachi F-2500 fluorescence spectrophotometer with a Xe lamp as the light source. All spectra were recorded at room temperature. The thermogravimetric (TG) and differential thermal analyses (DTA) were performed with a SDT Q600 thermal analyser, with a heating rate of 10 K min^{-1} and N_2 carrier gas with a flow rate of 220 ml min^{-1}.

3. Experimental results and analyses

Figure 1 shows SEM micrographs of the surfaces of the AAMs. A highly ordered nanopore array with a close-packed hexagonal structure can clearly be observed for the AAM_C and the AAM_S, while the morphology of the AAM_P appears to be disordered. The nanopore size is about 40 nm for the AAM_C and 20 nm for the AAM_S in diameter.

The PL spectra of the AAM_C, AAM_S and AAM_P are shown in figure 2. It has been found that the emission behaviours of the AAMs can be obviously affected by the type of electrolyte. The PL intensity of the AAM_C is the highest compared to those of the AAM_S and AAM_P. Under excitation by the 320 nm line of a Xe lamp, the AAM_C shows a strong

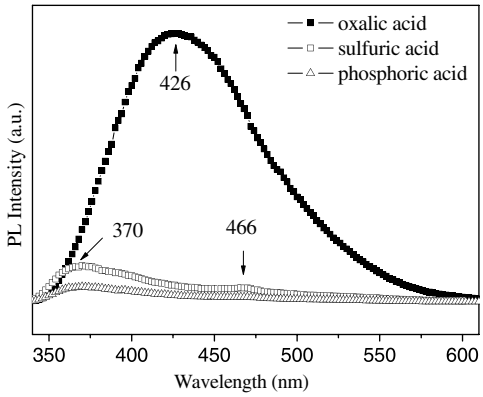

Figure 2. The PL spectra of the AAM_C, AAM_S and AAM_P. The PL spectra are excited at 320 and a 350 nm filter is used.

blue band at 426 nm and the AAM_S and the AAM_P have only very weak PL emission in the wavelength range from 340 to 610 nm. The AAM_S and the AAM_P show similar PL bands at 370 nm, which is different from the AAM_C. A weak peak located at 466 nm appears at the PL spectra of the AAM_S and the AAM_P. This means the light-emission processes in the AAM_S and the AAM_P are quite different from the AAM_C. This assumption is also supported by the following experimental results for the annealing treatment.

The PL spectra of the AAM_S, the AAM_P and the AAM_C before and after annealing at different temperatures for 4 h in N_2 are shown in figure 3. The PL results in figure 3 clearly reveal the evolution of the luminescence characteristics with the AAM structures, demonstrating the effects of the high-temperature annealing. The PL spectra of AAM_S and AAM_P have different line-shapes and annealing behaviour from the AAM_C. From figures 3(a) and (b), the intensity of this PL band increases with elevated annealing temperature and reaches a maximum for the sample annealed at about 300 °C, but decreases with a further increase in annealing temperature. Meanwhile the PL of the AAM_C shows a strong blue band after annealing and reaches a maximum at about 500 °C, as shown in figure 3(c). We may speculate that the AAM_S and the AAM_P have emission processes which are quite different from that of the AAM_C.

Investigation of the Gaussian fitting of PL spectra excited at 320 nm before and after annealing at 500 °C can help us understand the PL behaviour of the AAM_C. All the obtained spectra can be decomposed in three Gaussian distributions. Figure 3(d) shows the band maxima at 398 nm, 435 nm, and 473 nm, respectively. The inset of figure 3(d) shows the band maxima at 406 nm, 444 nm, and 478 nm, respectively. These results suggest that there might be three mechanisms for the PL of AAM_C. They arise from different defect centres coexisting in the alumina membrane.

Though there are many studies concerning the luminescence mechanisms of AAM, up to now the optical nature of AAMs is still ambiguous. Li *et al* [12] reported that the PL of AAM prepared in $C_2H_2O_4$ and H_2SO_4 have the same origin. Our results indicate clearly that there are two mechanisms for the PL of the AAM_S and the AAM_P and three mechanisms for the PL of AAM_C. The anodization process is a balance procedure, and there exist two opposite processes: the forming of the anodic aluminium films and the dissolving of the films [15]. Oxygen ions transform from OH^- in the electrolyte and migrate through the barrier layer under a high electric field (about 10^{-7} V cm^{-1}) by a vacancy mechanism [16]; this implies that many

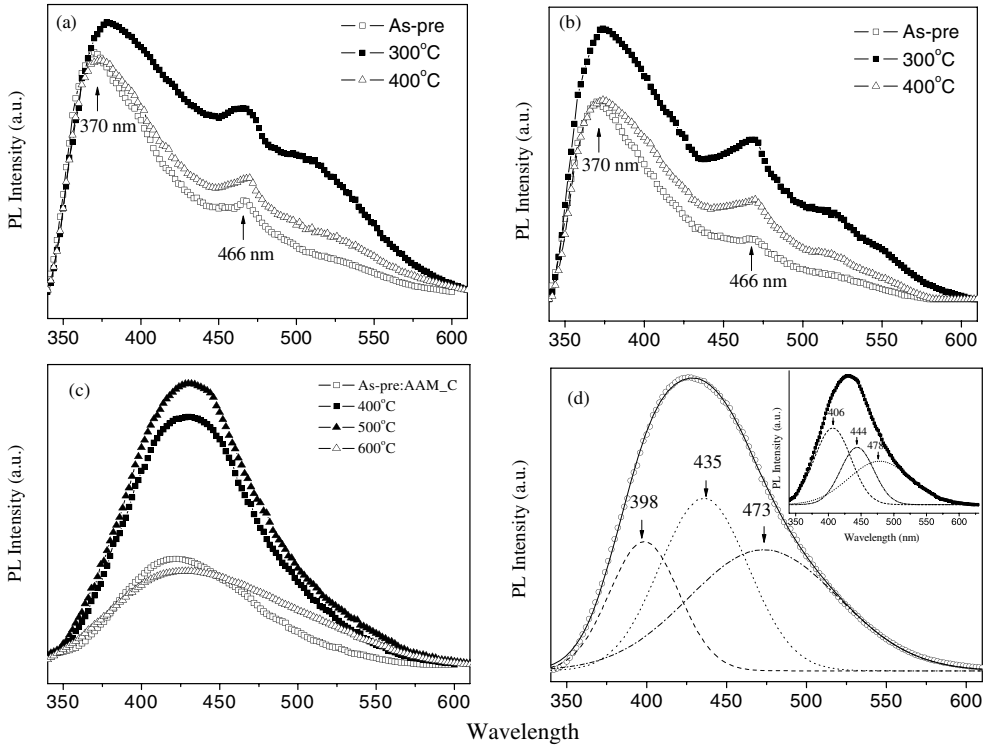

Figure 3. The PL spectra of (a) the AAM_S, (b) the AAM_P and (c) the AAM_C annealed at different temperatures for 4 h in N_2 excited at 320 nm. (d) The PL spectra of the as-prepared AAM_C and Gaussian fit band with three peaks. The inset (d) shows the PL spectra of the AAM_C annealed at 500 °C for 4 h in N_2 and Gaussian fit band with three peaks. The excitation wavelength is 320 nm and a 350 nm filter is used.

oxygen vacancies exist in the AAMs. The F and F^+ centres are produced from partial oxygen vacancies remaining in the AAM membrane formed [16]. The presence of oxygen vacancies has generally been considered to be responsible for the PL of anodic alumina [7, 9, 16]. Huang *et al* [10, 16] correlated the blue PL of AAM_C with F centres and F^+ centres. The density of the F centres is the largest on the surface, showing a blue PL band around 460 nm. It has also been reported that there exists a large number of F centres, and that the PL peak is located at 2.9 eV (430 nm) in crystalline alumina [17]. Considering the microstructural difference between AAMs, we believe that the luminescence centres located at 466 nm for the AAM_S and the AAM_P and at 435 nm for the AAM_C are intimately connected with the F centres. Electron paramagnetic resonance (EPR) measurements of the AAM_C demonstrate that an obvious EPR signal with a *g* factor of 2.0085 appears in the EPR spectrum [7], and that the alumina nanotube formed in sulfuric acid solution has been reported to have a similar EPR signal with a Landé *g* value of 2.0071 [18]. This EPR signal has been reported and attributed to F^+ centres [7]. Du *et al* [7] and Li *et al* [9] have attributed the blue emission band to the singly ionized oxygen vacancies (F^+ centres) in AAM_C; Huang *et al* [18] and Wu *et al* [19] have reported that the luminescence characteristics of the sulfuric AAMs can come from F^+ centres [19]. In crystalline Al_2O_3, it has been proven experimentally that the F^+ centre can emit a PL peak at about 413 nm (3.0 eV) [10]. Therefore, we may infer that the luminescence centres located at 370 nm, AAM_S and AAM_P, and at 398 nm, AAM_C, might be related to

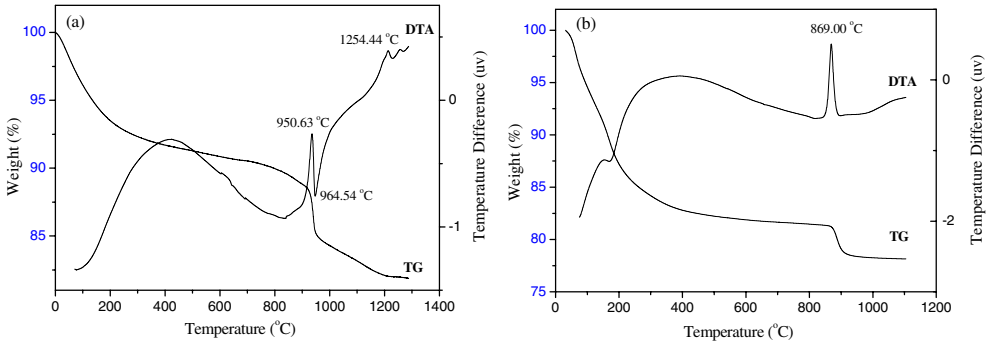

Figure 4. TG–DTA curve of (a) the AAM_S, (b) the AAM_C.

the F^+ centres. A large PL intensity corresponds to a large concentration of oxygen vacancies. The AAM_C has the most oxygen vacancies and the PL intensity is the strongest.

In this paper, we have also found that the luminescence characteristics of the AAM_S and AAM_P clearly show differences from those of AAM_C. Huang *et al* [18] report that alumina nanotubes formed in 15 wt% sulfuric acid solution show a strong PL band at 400 nm, which they rule out to being due to the SO_4^{2-} group. Yamamoto [8] and Gao *et al* [13] have proposed that the oxalic impurities incorporated in the AAMs can be transformed into luminescent centres by a high-electric-field setup inside the pores, showing a blue PL band around 470 nm. It is reasonable to assume that the incorporated oxalic impurities existing in the AAM_C would have important influences on their optical properties.

In order to reveal the presence of impurities, DTA and TG analysis of AAM_S and AAM_C were used. Figure 4(a) shows the TG–DTA result of the AAM_S. The DTA curve shows a very sharp exothermic peak centred at 950 °C and a successive distinct endothermic peak is observed at 964 °C. Another slightly broader exothermic reaction is observed at 1229 °C. The TG curve consists of three sections, consisting of a gradual weight loss of 11.425% from room temperature up to 930 °C, followed by a very pronounced weight loss of 3.385% at about 950 °C, coincident with the first exothermal event. In the third section between 964 and 1300 °C the sample gradually loses 3.301 mass%. Above 1300 °C, the sample weight remains constant. The complete thermal process can be summarized as follows [20]: the AAM_S contains bound and structural hydroxyl species which are responsible for the initial gradual weight loss as the PAA loses water with increasing temperature. At 950 °C the amorphous alumina crystallizes into γ-alumina. This event is linked to a rapid exothermic weight loss caused by the decomposition of the sulphate anions with the release of SO_2 and O_2. The release of SO_2 from PAA continues up to 1230 °C. At 1229 °C the alumina undergoes a phase transition to the stable phase corundum.

Figure 4(b) shows the TG–DTA curve for the AAM_C. DTA results show that one endothermic peak exists at around 171 °C. It is associated with continuous removal of the structural water in the hydroxide and oxy-hydroxide of aluminium [21]. Typically, the AAM_C yields an exothermic peak at 869 °C, due to the amorphous $\rightarrow$ γ-Al_2O_3 phase transformation. Furthermore, a broad exothermic peak is observed to occur above 994 °C, due to the θ-Al_2O_3 $\rightarrow$ α-Al_2O_3 phase transformation [20]. Four weight loss regions are observed in the TG curve (figure 4(b)). The weight loss for the first section from room temperature to 100 °C, about 5.448%, is mainly attributed to the desorption of weakly bound water from the surface and the inner walls of nanopores. The water is referred to the physically absorbed one. In the second process from 100 to 200 °C, the weight loss is about 7.423%, which may come from desorption

of chemisorbed water molecules. The third section from 200 to 852 °C accompanying a mass loss of about 5.780% has a relation to the decomposition of oxalic impurities, because the decomposition of metal oxalates is believed to occur at a temperature higher than 350 °C [22]. The long temperature range for this section indicates that quite a number of oxalic ions are incorporated within the structure of the porous anodic alumina films. The fourth section, from 850 to 940 °C, is a typical TG feature indicating a strong phase transition. It is concluded that the AAM_C experiences a transition from amorphous to γ phase. During this transformation, the –OH groups in the crystalline structure of γ-Al_2O_3 [21] will be lost, which results in the weight loss. When the AAM_C begins to transform into crystalline Al_2O_3 above 800 °C, the periodic and ordered arrangement of the Al and O atoms (or oxygen vacancies) contributes to the formation of stable carboxylic impurities [11], such as aluminium–carboxylate complex in AAM_C, which also results in a weight loss. During the annealing treatment, the oxalic impurities that are incorporated would decompose. A large number of =CO groups would form and the number of PL centres generated from the decomposition of oxalic impurities would enlarge with the increase in the annealing temperature, resulting in the PL intensities increasing. The decomposition of oxalic impurities keeps increasing with the annealing temperature until the largest degree of decomposition at 700 °C [11]. From figure 4, we may arrive at the conclusion that the impurities strongly influence the structure and crystallization of the AAMs, causing it to transform into γ-alumina at about 950 °C for AAM_S, approximately 80 K higher than for AAM_C. This agreement makes us believe that the 473 nm PL band originates from the oxalic impurities incorporated in the AAMs.

4. Conclusions

We have investigated the blue emission property of the AAM_C, AAM_S and AAM_P and their annealing behaviour of the blue emission band. The electrolyte has a large influence on the light-emitting property of an anodic alumina membrane. We have attributed the blue emission to the F^+ centres and the F centre in the AAM_S and AAM_P. DTA and TG analysis indicates that the impurities strongly influence the crystallization of the AAMs. Oxalic ions incorporated into the AAM_C have been proved by the TG experiment, and the oxalic ions have important influences on forming the optical centres of AAM_C. This suggests that the blue emission band in AAM_C originates from the coactions of the F^+ centres, the F centre and the luminescent centres transformed from oxalic impurities. The results reveal that the luminescence properties of the PAA films are very sensitive to their chemical and structural characteristics, which depend mainly on their preparation conditions. The present work improves the understanding of the PL property of the AAMs formed in different acids.

References

[1] Setch S and Miyata A 1932 *Sci. Pap. Inst. Phys. Chem. Res.* **19** 237
[2] Masuda H and Fukuda K 1995 *Science* **268** 1466
[3] Li A P, Müller F, Birner A, Nielsch K and Gösele U 1998 *J. Appl. Phys.* **84** 6023
[4] Suh J S and Lee J S 1999 *Appl. Phys. Lett.* **75** 2047
[5] Goh C, Coakley K M and Michael D 2005 *Nano Lett.* **5** 1545
[6] Jessensky O, Müller F and Gösele U 1998 *Appl. Phys. Lett.* **72** 1173
[7] Du Y, Cai W L, Mo C M, Chen J, Zhang L D and Zhu X G 1999 *Appl. Phys. Lett.* **74** 2951
[8] Yamamoto Y, Baba N and Tajima S 1981 *Nature* **289** 572
[9] Li Y, Li G H, Meng G W, Zhang L D and Phillipp F 2001 *J. Phys.: Condens. Matter* **13** 2691
[10] Huang G S, Wu X L, Mei Y F, Shao X F and Siu G G 2003 *J. Appl. Phys.* **93** 582
[11] Xu W L, Zheng M J, Wu S and Shen W Z 2004 *Appl. Phys. Lett.* **85** 4364

[12] Li G H, Zhang Y, Wu Y C and Zhang L D 2003 *J. Phys.: Condens. Matter* **15** 8663
[13] Gao T, Meng G W and Zhang L D 2003 *J. Phys.: Condens. Matter* **15** 2071
[14] Huang G S, Wu X L, Siu G G and Chu P K 2006 *Solid State Commun.* **137** 621
[15] Wang H and Wang H W 2005 *Appl. Surf. Sci.* **249** 151
[16] Huang G S, Wu X L, Yang L W, Shao X F, Siu G G and Chu P K 2005 *Appl. Phys.* A **81** 1345
[17] Draeger B G and Summers G P 1979 *Phys. Rev.* B **19** 1172
[18] Huang G S, Wu X L, Kong F, Cheng Y C, Siu G G and Chu P K 2006 *Appl. Phys. Lett.* **89** 073114
[19] Wu J H, Wu X L, Tang N, Mei Y F and Bao X M 2001 *Appl. Phys.* A **72** 735
[20] Kirchner A, MacKenzie K J D, Brown I W M, Kemmitt T and Bowden M E 2007 *J. Member. Sci.* **287** 264
[21] Li J G and Sun X D 2000 *Acta Mater.* **48** 3103
[22] Sun X Y, Xu F Q, Li Z G and Zhang W H 2006 *J. Lumin.* **121** 588